Anal. Chem. **2006,** *78,* 3104−3112

Determination of the Structure and Orientation of Organic Molecules Tethered to Flat Graphitic Carbon by ATR-FT-IR and Raman Spectroscopy

Franklin Anariba,[†] Umamaheswari Viswanathan,[‡] David F. Bocian,*[,†] and Richard L. McCreery*[,‡]

Department of Chemistry, University of California, Riverside, California 92521, and Department of Chemistry, The Ohio State University, 100 West 18th Avenue, Columbus, Ohio 43210

Mono- and multilayers of nitroazobenzene (NAB), azobenzene (AB), nitrobiphenyl (NBP), biphenyl (BP), and fluorene (FL) were covalently bonded to flat pyrolyzed photoresist films (PPF) by electrochemical reduction of their diazonium derivatives. The structure and orientation of the molecular layers were probed with ATR-FT-IR and Raman spectroscopy. A hemispherical germanium ATR element used with p-polarized light at 65° incidence angle yielded high signal/noise IR spectra for monolayer coverage of molecules on PPF. The IR spectra are dominated by in-plane vibrational modes in the 1000−2000-cm^{-1} spectral range but also exhibit weaker out-of-plane deformations in the 650−1000-cm^{-1} region. The average tilt angle with respect to the surface normal for the various molecules varied from 31.0 ± 4.5° for NAB to 44.2 ± 5.4° for FL with AB, NBP, and BP exhibiting intermediate adsorption geometries. Raman intensity ratios of NAB and AB for p- and s-polarized incident light support the conclusion that the chemisorbed molecules are in a predominantly upright orientation. The results unequivocally indicate that molecules electroreduced from their diazonium precursors are not chemisorbed flat on the PPF surface, but rather at an angle, similar to the behavior of Au/thiol self-assembled monolayers, Langmuir−Blodgett films, and porphyrin molecules chemisorbed thermally on silicon and PPF from alkyne and alkene precursors.

Recent interest in molecular electronic concepts and devices has stimulated investigations of bonding between conducting "contacts" and a variety of molecules, including aliphatic and aromatic hydrocarbons, heterocyclic molecules, and conducting polymers. To understand electron transport across molecular junctions consisting of single molecules or groups of molecules oriented between conducting contacts, it is necessary to characterize the nature and geometry of the molecule/conductor bond. The current report discusses aromatic molecules bonded to a graphitic carbon surface, which are the basis of one of the reported paradigms for determining electron transport mechanisms through molecular junctions.

Covalent attachment of a variety of molecules to graphitic surfaces via aryldiazonium ion reduction has been reported by various investigators.[1−13] The highly reactive phenyl radicals produced electrochemically from diazonium reagents lead to densely packed monolayers on carbon, with the formation of a strong and stable C−C bond between a phenyl ring and the substrate. Carbon surfaces modified via diazonium electroreduction have been used in a number of different types of studies including adhesion promotion in carbon fiber composites,[3,4] electroanalysis and electrocatalysis,[12,14−16] electrode kinetics,[8,15−17] and nanoscale patterning[18] and investigations of current−voltage behavior of molecular junctions.[19−29]

* To whom correspondence should be addressed. E-mail: David.Bocian@ucr.edu; Mccreery.2@osu.edu.

[†] University of California.

[‡] The Ohio State University.

(1) Delamar, M.; Hitmi, R.; Pinson, J.; Saveant, J. M. *J. Am. Chem. Soc.* **1992**, *114*, 5883−5884.
(2) Allongue, P.; Delamar, M.; Desbat, B.; Fagebaume, O.; Hitmi, R.; Pinson, J.; Saveant, J. M. *J. Am. Chem. Soc.* **1997**, *119*, 201−207.
(3) Delamar, M.; Desarmot, G.; Fagebaume, O.; Hitmi, R.; Pinson, J.; Saveant, J. *Carbon* **1997**, *35*, 801−807.
(4) Coulon, E.; Pinson, J.; Bourzat, J.-D.; Commercon, A.; Pulicani, J.-P. *Langmuir* **2002**, *17*, 7102−7106.
(5) Kariuki, J. K.; McDermott, M. T. *Langmuir* **1999**, *15*, 6534−6540.
(6) Kariuki, J. K.; McDermott, M. T. *Langmuir* **2001**, *17*, 5947−5951.
(7) Chen, P.; Fryling, M.; McCreery, R. L. *Anal. Chem.* **1995**, *67*, 3115.
(8) Chen, P.; McCreery, R. L. *Anal. Chem.* **1996**, *68*, 3958.
(9) Itoh, T.; McCreery, R. L. *J. Am. Chem. Soc.* **2002**, *124*, 10894−10902.
(10) Saby, C.; Ortiz, B.; Champagne, G. Y.; Belanger, D. *Langmuir* **1997**, *13*, 6805−6813.
(11) Ortiz, B.; Saby, C.; Champagne, G. Y.; Belanger, D. *J. Electroanal. Chem.* **1998**, *455*, 75−81.
(12) Downard, A. J.; Roddick, A. D. *Electroanalysis* **1995**, *7*, 376−378.
(13) Downard, A. J. *Electroanalysis* **2000**, *12*, 1085−1096.
(14) Downard, A. J. *Langmuir* **2000**, *16*, 9680−9682.
(15) DuVall, S.; McCreery, R. L. *Anal. Chem.* **1999**, *71*, 4594−4602.
(16) DuVall, S.; McCreery, R. L. *J. Am. Chem. Soc.* **2000**, *122*, 6759−6764.
(17) DuVall, S.; Yang, H.-H.; McCreery, R. L. In *Proceedings of the Electrochemical Society*; Leddy, J., Vanysek, P., Porter, M. D., Eds.; Electrochemical Society: Pennington, NJ, 1999; Vol. 99, pp 33−36.
(18) Brooksby, P.; Downard, A. J. *Langmuir* **2005**, *21*, 1672.
(19) Ranganathan, S.; Steidel, I.; Anariba, F.; McCreery, R. L. *Nano Lett.* **2001**, *1*, 491−494.
(20) Anariba, F.; McCreery, R. L. *J. Phys. Chem. B* **2002**, *106*, 10355−10362.
(21) Solak, A. O.; Ranganathan, S.; Itoh, T.; McCreery, R. L. *Electrochem. Solid State Lett.* **2002**, *5*, E43−E46.
(22) McCreery, R. L.; Dieringer, J.; Solak, A. O.; Snyder, B.; Nowak, A.; McGovern, W. R.; DuVall, S. *J. Am. Chem. Soc.* **2003**, *125*, 10748−10758.
(23) McCreery, R. L.; Dieringer, J.; Solak, A. O.; Snyder, B.; Nowak, A. M.; McGovern, W. R.; DuVall, S. *J Am Chem Soc* **2004**, *126*, 6200.
(24) Nowak, A. M.; McCreery, R. L. *Anal. Chem.* **2004**, *76*, 1089−1097.
(25) McGovern, W. R.; Anariba, F.; McCreery, R. L. *J. Electroanal. Chem. Soc.* **2004**, *152*, E176.
(26) McCreery, R. L. *Chem. Mater.* **2004**, *16*, 4477−4496.
(27) Nowak, A. M.; McCreery, R. L. *J. Am. Chem. Soc.* **2004**, *126*, 16621−16631.

10.1021/ac052042h CCC: $33.50
Published on Web 03/30/2006

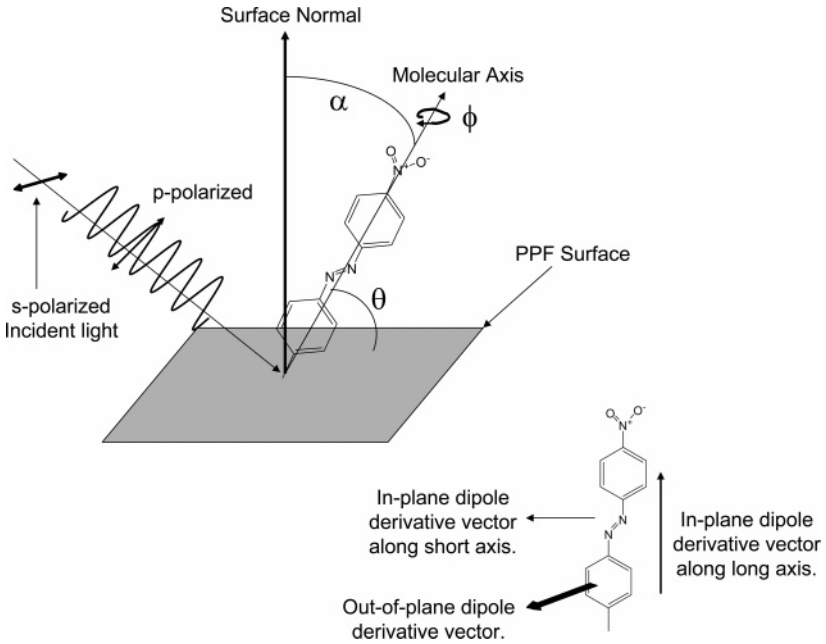

Figure 1. Relationship between incident light and chemisorbed NAB molecule. The incident angle for IR light in the GATR configuration was 65° relative to the surface normal. Also shown are the dipole derivative vectors for NAB. ϕ is zero when the transition dipole along the short axis of the molecule is parallel to the surface plane.

The formation of monolayers and multilayers of various diazonium salts has been demonstrated by systematically varying the charge (Q), solution concentration (M), and deposition time (t). The ensuing diazonium films have been characterized by voltammetry,[2,3,11,15−17,30] X-ray photoelectron spectroscopy,[2,11] time-of-flight secondary ion mass spectroscopy,[31] atomic force microscopy,[18,30,32,33] Raman spectroscopy,[9,34] and Fourier transform infrared reflection−absorbance spectroscopy.[5,6,35] Surface spectroscopic techniques such as FT-IR and Raman can provide valuable information about the structure and orientation of films chemisorbed onto surfaces.[36] The molecular orientation of self-assembled monolayers deposited onto metal surfaces has been previously determined by infrared spectroscopy.[37−41] In addition, FT-IR has been employed to obtain the orientation of Langmuir−Blodgett films[42] physisorbed to various metals and glass and the adsorption geometry of porphyrin monolayers covalently bonded to silicon surfaces.[43−45] The optical properties of carbon, particularly its strong absorption coefficient in the UV−visible−IR regions and its inability to support electromagnetic field enhancement in surface-enhanced Raman spectroscopy, make it much less amenable than metals to surface spectroscopy. As a result, vibrational studies of adsorbed films on graphitic surfaces have been limited. The first FT-IR studies of molecules on glassy carbon (GC) were reported for physisorbed $Cu_3(Fe(CN)_6)_2$ films.[46−48] In subsequent work, the quantitative aspects of infrared external reflection spectroscopy for the characterization of thin poly(methyl methacrylate) films on GC were reported,[49] with the carbonyl stretch observed for a film thickness down to 7.8 nm.

The infrared absorption characteristics of molecular adlayers on carbon substrates differ from those of adlayers on metals in that image dipoles and the associated surface selection rules do not significantly affect the intensities of the vibrational modes. In particular, the IR absorption observed using p-polarized incident light at near-glancing incidence will be largest for vibrations with dipole derivative vectors more parallel to the surface normal, even if an image dipole is weak or absent (Figure 1). IR absorption will also be observed using s-polarized light; however, the largest absorption will occur for vibrations whose dipole derivatives are more parallel to the plane of the surface. The relative IR intensities of vibrations whose dipole derivatives are oriented along different molecular axes can be used to determine the orientation of the

(28) McCreery, R. L. *Interface* **2004**, *13*, 46.
(29) Anariba, F.; Steach, J. K.; McCreery, R. L. *J. Phys. Chem. B* **2005**, *109*, 11163.
(30) Brooksby, P.; Downard, A. J. *Langmuir* **2004**, *20*, 5038.
(31) Combellas, C.; Knaoufi, F.; Pinson, P.; Podvorica, F. *Langmuir* **2005**, *21*, 280.
(32) Anariba, F.; DuVall, S. H.; McCreery, R. L. *Anal. Chem.* **2003**, *75*, 3837−3844.
(33) Brooksby, P.; Downard, A. J. *J. Phys. Chem. B* **2005**, *109*, 8791.
(34) Liu, Y.-C.; McCreery, R. L. *J. Am. Chem. Soc.* **1995**, *117*, 11254.
(35) Adenier, A.; Cabet-Deliry, E.; Chausse, A.; Griveau, S.; Mercier, F.; Pinson, J.; Ul-Vautrin, C. *Chem. Mater.* **2005**, *17*, 491.
(36) Greenler, R. G. *J. Chem. Phys.* **1966**, *44*, 310.
(37) Allara, D. L.; Nuzzo, R. G. *Langmuir* **1985**, *1*, 52.
(38) Ulman, A.; Eilers, J.; Tillman, N. *Langmuir* **1989**, *5*, 1147.
(39) Shaporenko, A.; Cyganik, P.; Buck, M.; Ulman, A.; Zharnikov, M. *Langmuir* **2005**, *21*, 8204.
(40) Porter, M. D.; Bright, T. B.; Allara, D. L.; Chidsey, C. E. D. *J. Am. Chem. Soc.* **1987**, *109*, 3559−3568.
(41) Alves, C. A.; Porter, M. D. *Langmuir* **1993**, *9*, 3507.
(42) Hulshof, J.; Feringa, B.; Schoondorp, M.; Schouton, A. J. *Langmuir* **1992**, *8*, 1825.
(43) Yasseri, A.; Syomin, D.; Malinovskii, V.; Loewe, R.; Lindsey, J.; Zaera, F.; Bocian, D. *J. Am. Chem. Soc.* **2004**, *126*, 11944.
(44) Wei, L.; Syomin, D.; Loewe, R.; Lindsey, J. S.; Zaera, F.; Bocian, D. F. *J. Phys. Chem. B* **2005**, *109*, 6323.
(45) Yasseri, A.; Syomin, D.; Loewe, R.; Lindsey, J.; Zaera, F.; Bocian, D. *J. Am. Chem. Soc.* **2004**, *126*, 15603.
(46) Porter, M. D.; Karweik, D. H.; Kuwana, T.; Theis, W. B.; Norris, G. B.; Tiernan, T. O. *Appl. Spectrosc.* **1984**, *38*, 11−16.
(47) Datta, M.; Freeman, J.; Jansson, R. *Spectrosc. Lett.* **1985**, *18*, 273.
(48) Datta, M.; Robert, E. W.; Freeman, J. *Spectrosc. Lett.* **1986**, *19*, 129.
(49) Porter, M. D.; Bright, T. B.; Allara, D. L. *Anal. Chem.* **1986**, *58*, 2461−2465.

molecules on the surface. This is illustrated in Figure 1, which uses nitroazobenzene (NAB, one of the molecules of interest in the present study) as an example. For this molecule, the relative intensities of the vibrations polarized along the long axis versus those polarized out of the plane of the molecule can be used to obtain the angle between the surface and the long molecular axis (θ), as expressed in eqs 1−3. Similarly, the relative intensities of modes polarized along the short axis versus the out-of-plane vibrations can be used to obtain the rotation angle about the long axis of the molecule (ϕ), as expressed in eqs 4 and 5:[36,37,50−52]

$$(I^{\mathrm{la}}_{\mathrm{in-plane}}/I_{\mathrm{out-of-plane}})_{\mathrm{monolayer}} = (I^{\mathrm{la}}_{\mathrm{in-plane}}/I_{\mathrm{out-of-plane}})_{\mathrm{iso}}\ (\tan^2\theta/\cos^2\phi) \quad (1)$$

$$\theta = \tan^{-1}\{[(I^{\mathrm{la}}_{\mathrm{in-plane}}/I_{\mathrm{out-of-plane}})_{\mathrm{monolayer}}\ (\cos^2\phi)/(I^{\mathrm{la}}_{\mathrm{in-plane}}/I_{\mathrm{out-of-plane}})_{\mathrm{iso}}]^{1/2}\} \quad (2)$$

$$\alpha = 90 - \theta \quad (3)$$

$$(I^{\mathrm{sa}}_{\mathrm{in-plane}}/I_{\mathrm{out-of-plane}})_{\mathrm{monolayer}} = (I^{\mathrm{sa}}_{\mathrm{in-plane}}/I_{\mathrm{out-of-plane}})_{\mathrm{iso}}\ (\tan\phi)^2 \quad (4)$$

$$\phi = \tan^{-1}\{[(I^{\mathrm{sa}}_{\mathrm{in-plane}}/I_{\mathrm{out-of-plane}})_{\mathrm{monolayer}}/(I^{\mathrm{sa}}_{\mathrm{in-plane}}/I_{\mathrm{out-of-plane}})_{\mathrm{iso}}]^{1/2}\} \quad (5)$$

where I is the relative infrared intensity for a given spectrum, I^{la} refers to the relative infrared intensities for modes with dipole derivatives along the long axis of the molecule, I^{sa} is the relative infrared intensities along the short axis of the molecule, I_{iso} refers to isotropically oriented material, θ is the angle between the surface and the long molecular axis, α is the average tilt angle of the molecule relative to the surface normal, and ϕ is the rotation angle about the long axis of the molecule.

Raman spectroscopy with polarized incident laser light has also been used to determine the orientation of molecules adsorbed onto highly ordered pyrolytic graphite (HOPG)[53] and polished GC[54] and to probe the orientation of single-wall carbon nanotubes.[55,56] The main factor affecting the Raman scattering from carbon surfaces is the relationship between the incident electric field and the orientation of the molecules. In the case of metal phthalocyanines adsorbed on the basal plane of HOPG, the resonance Raman scattering intensity was maximized when the electric field vector of the incident light was parallel to the plane of the macrocycle.[53] For the case of NAB, shown in Figure 1, we expect maximum Raman intensity when the incident electric field is parallel to the long axis of the molecule, which has the largest polarizability.

Table 1. Modification Conditions and Film Thicknesses

molecule	deposition potential, V[a]	thickness, nm[c]	no. of samples[d]
NAB	0.0 (1)[b]	1.0	2
NAB (1.9)	−0.2 (1)	1.9	5
NAB (4.5)	−0.6 (4)	4.5	4
AB	−0.2 (1)	1.2	2
AB	−0.6 (4)	2.1	1
NBP (1.7)	−0.4 (1)	1.7	5
NBP (4.2)	−0.6 (10)	4.2	4
BP	−0.8 (1)	1.6	4
FL	−0.8 (1)	1.7	5
NAB	physisorbed		1
NBP	physisorbed		2
BP	physisorbed		1
FL	physisorbed		3
PANI	see text	6.0[e]	
PANI	see text	50[e]	

[a] Negative potential limit for derivatization scan, stated vs Ag/Ag^+ (0.1 M). All scans started at +0.4 V vs Ag/Ag^+, at a scan rate of 0.2 V/s. [b] Number in parentheses indicates number of derivatization cycles. [c] AFM thickness established by "scratching" technique.[32] [d] Refers to independently prepared mono- or multilayers. [e] Thickness determined with ellipsometry, with $n = 1.8997$ and $k = 0.64$

The current investigation was undertaken to determine the molecular orientations of monolayers of NAB, azobenzene (AB), nitrobiphenyl (NBP), biphenyl (BP), fluorene (FL), and multilayers of NAB, AB, and NBP on flat graphitic carbon. The orientations were obtained by using a combination of polarized IR and Raman spectroscopy. The studies confirm the molecular structure following chemisorption as well as the average tilt angle with respect to the surface. These results were correlated with the conductivity of molecular electronic junctions made from similar monolayers, which have been previously reported.[29]

EXPERIMENTAL SECTION

Preparation of Pyrolyzed Photoresist Films. The procedure for preparing pyrolyzed photoresist films (PPF) has been described previously.[57,58] Briefly, positive photoresist AZ P4330-RS (AZ Electronic Materials, Somerville, NJ) was spin-coated onto clean silicon at 6000 rpm for 30 s before a programmed heat treatment to 1000 °C for 60 min under flowing forming gas (95% N_2 + 5% H_2 at ~100 mL/min). As noted previously, PPF is similar in properties and conductivity to GC, with primarily sp^2-hybridized bonding.[57,58] The PPF surface is flat (<5 Å rms by AFM), with a presumably disordered mix of basal and edge sites.

Surface Derivatization. PPF surfaces were modified by diazonium reduction as described previously,[22] with Ag/Ag^+ (0.1 M $AgNO_3$) electrode (Bioanalytical Systems), calibrated to the $E_{1/2}$ of ferrocene acting as the reference electrode. Tetrafluoroborate diazonium salts were prepared from 4-amino-4′-nitroazobenzene, 4-aminoazobenzene, 4-amino-4′-nitrobiphenyl, 4-aminobiphenyl, and 4-aminofluorene according to previously established procedures.[22,32] Potential scans for the various molecules are described below and summarized in Table 1. The thickness of the molecular layers was verified for separate samples treated with the same procedure using AFM "scratching".[32] A submonolayer

(50) Painter, P. C.; Coleman, M. M.; Koenig, J. L. *The Theory of Vibrational Spectroscopy and Its Application to Polymeric Materials*; Wiley: New York, 1982.
(51) Harrick, N. J.; Mirabella, F. M. *Internal Reflection Spectroscopy: Review and Supplement*; Harrick Scientific Group: New York, 1985.
(52) Zaera, F. *Int. Rev. Phys. Chem.* **2002**, *21*, 433.
(53) Zhao, J.; McCreery, R. L. *Langmuir* **1995**, *11*, 4036.
(54) Liu, Y.-C.; McCreery, R. L. *Anal. Chem.* **1997**, *69*, 2091.
(55) Azoulay, J.; Debarre, A.; Richard, A.; Tchenio, P.; Bandow, S.; Iijima, S. *Chem. Phys. Lett.* **2000**, *331*, 347.
(56) Yu, Z.; Brus, L. *J. Phys. Chem. B* **2001**, *105*, 1123.
(57) Ranganathan, S.; McCreery, R. L.; Majji, S. M.; Madou, M. *J. Electrochem. Soc.* **2000**, *147*, 277−282.
(58) Ranganathan, S.; McCreery, R. L. *Anal. Chem.* **2001**, *73*, 893−900.

of NAB (average 1.0 nm thick) was bonded to PPF by a single cycle at 0.2 V/s from +0.4 to 0.0 V versus Ag/Ag^+(0.1 M $AgNO_3$) and back to +0.4 V. Monolayers of NAB, BP, FL, and AB as well as multilayers of NAB, AB, and NBP were deposited with similar scans in the respective diazonium ion solutions using the conditions summarized in Table 1. To distinguish monolayers from multilayers, the AFM determined molecular layer thickness in nm appears in parentheses, e.g. NAB(1.9). A polyaniline (PANI) thin film was prepared on PPF by cycling the potential between −0.2 and 1.2 V in a 0.2 M solution of aniline in 0.5 M H_2SO_4 at 0.2 V/s; a thicker film was formed by cycling in a 0.1 M aniline/0.25 M H_2SO_4 solution at 0.05 V/s. After derivatization, the samples were immediately rinsed with acetonitrile and dried with an argon stream.

IR and Raman studies were also performed on physisorbed NAB, NBP, BP, and FL monolayers (not their diazonium salts), which were obtained by spontaneous adsorption from freshly prepared 0.5 mM solutions in anhydrous acetonitrile (Sigma-Aldrich). For the IR studies, PPF samples were immersed in solutions of NAB, NBP, BP, and FL for periods of 2, 10, 10, and 20 min, respectively, removed, and allowed to dry in air. Because no attempt was made to achieve comparable coverages for physisorbed molecules, the IR intensities vary significantly for the physisorbed samples. For the Raman experiments on NAB, spontaneous physisorption yielded too weak a Raman signal to be useful, and films formed by drying aliquots of the NAB in acetonitrile deposited on PPF produced very irreproducible Raman intensities. Spin coating of 1−5 mM solutions of NAB in acetonitrile resulted in more even coverage and reproducible Raman intensities.

FT-IR Spectroscopy. FT-IR spectra of the organic molecules in both solid and monolayer forms were collected at room temperature (Bruker Tensor 27 FT-IR) with a spectral resolution of 4 cm^{-1} in all cases. The spectra of the solids were obtained in KBr pellets (∼1−5 wt %) using transmission mode and a room-temperature DTGS detector by averaging 32 scans. The IR spectra of monolayers of NAB, NBP, BP, and FL and multilayers of NAB, and NBP tethered to the graphitic surfaces were obtained using a Ge total reflection accessory (GATR; 65° incident angle relative to surface normal, Harrick Scientific) and a liquid N_2-cooled MCT detector averaging 256 scans. In the GATR accessory, the carbon substrates are positioned in contact with the flat surface of a hemispherical Ge crystal that functions as the ATR element. All spectra of the monolayers were obtained using p-polarized radiation. Before spectral analysis, each sample was thoroughly and gently cleaned with a Q-tip previously immersed in 2-butanone to ensure removal of particles. PPF spectra were obtained from clean unmodified surfaces and subtracted from monolayer/PPF spectra. Because the background subtraction procedure was not perfect due to sample variations, a manual correction was applied to produce a flat baseline. Spectral peak intensities were determined as peak height above the baseline. The reader is referred to our previous publications for additional experimental details.[43−45]

Raman Spectroscopy. Raman spectra of monolayers and multilayers of NAB and AB and films of PANI were collected with a custom-built line-focused *f*/2 Raman spectrometer (Chromex) and a thermoelectrically cooled (−85 °C) back-thinned CCD (Andor, 256 × 1024 pixels) described previously.[59] The excitation source was the 514.5-nm line of an argon ion laser (Coherent Innova 308). The power at the sample was 35 mW for incident angles of 0° and 45° and 110 mW for an incident angle of 75°. The higher power for 75° was used to keep the power density constant across the slit image at the PPF surface. All spectra were averages of 10 integrations having durations of 5 s each. Raman spectra of BP, FL, and NBP on PPF were too weak for useful analysis.

The laser beam was line-focused (5 mm × 50 μm) on the sample by a Powell lens, which was followed by a half-wave plate to control the laser polarization to be either s- or p-polarized at the PPF surface. A polarization scrambler was positioned along the collection axis, which was fixed at 45° relative to the incident laser axis. Spectrometer response to polarized light was verified by measuring known depolarization ratios for liquid benzene and CCl_4. In all spectra reported, the spectrum of unmodified PPF obtained under the same conditions of intensity and polarization was subtracted. A baseline correction was applied to all spectra, and peak center frequencies were measured using the "center X" function in Grams 32/AI, version 6.00 (Galactic Industries, Salem, NH). The Raman shift was calibrated with benzonitrile, and intensities were not corrected for instrument response. As discussed below, the Raman parameter relevant to the molecular orientation is the ratio of the intensity of a given Raman band with p-polarized incident laser light to that with s-polarized laser light. The ratio should not be confused with the depolarization ratio, which usually is applied to isotropic samples. In the current investigation, the intensity ratio was determined for the 1140-cm^{-1} band of NAB and the 1142-cm^{-1} band of AB because these bands have minimal interference from the Raman scattering of the carbon substrate. No polarization analyzers were used for the scattered light, and the only experimental parameter changed for a given intensity ratio measurement was the rotation of the half-wave plate.

Molecular Modeling. Molecular modeling was performed with Spartan'04, version 1.0.3,[60] using the density functional theory method B3LYP with basis set 6-31G*.

RESULTS

Infrared Spectroscopy. The IR spectra of the various samples were collected in the 650−4000-cm^{-1} range but are reported over only a 650−2000-cm^{-1} spectral range because only weak bands were observed above 2000 cm^{-1}. Figure 2 displays the FT-IR spectra of (a) raw NBP-modified PPF and (b) averaged raw PPF background ($N = 3$). Spectrum c is the difference spectrum of (a − b) while (d) is a NBP monolayer spectrum after applying a manual correction to create a flat baseline. Several PPF background spectra were obtained and averaged under the same conditions as the sample spectrum and then subtracted from the sample spectrum of interest. PPF background spectra showing considerable deviation from the spectrum of the sample of interest were not included in the average background spectrum. The procedure illustrated in Figure 2 was used to obtain all of the spectra of the chemisorbed and physisorbed molecules.

The IR spectra for solid NAB in a KBr pellet, a chemisorbed NAB monolayer on PPF, and NAB physisorbed onto PPF are

(59) Ramsey, J. D.; Ranganathan, S.; Zhao, J.; McCreery, R. L. *Appl. Spectrosc.* **2001**, *55*, 767−773.
(60) Spartan'04. Wavefunction Inc., Irvine, CA.

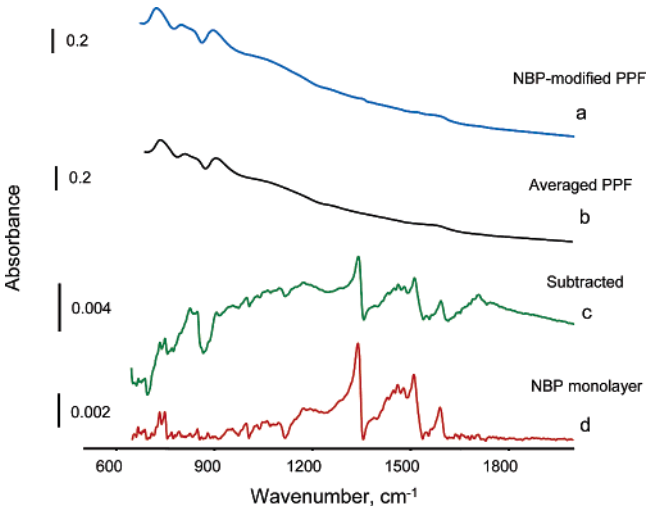

Figure 2. FT-IR spectra of (a) NBP-modified PPF and (b) averaged PPF. Spectrum c is the difference spectrum (a − b); spectrum d is that of NBP monolayer after applying a linear baseline correction.

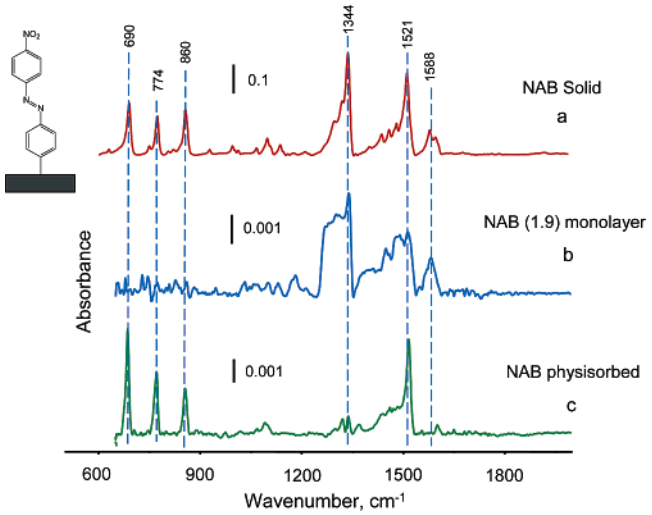

Figure 3. FT-IR spectra of (a) solid NAB in a KBr pellet, (b) the corresponding chemisorbed monolayer 1.9 nm thick, and (c) a physisorbed layer on PPF.

shown in Figure 3. Free NAB is a planar structure, whose infrared spectrum contains both in-plane and out-of-plane contributions, as summarized in Table 2. In-plane vibrations are responsible for peaks at 1344 (ν_s NO_2), 1521(ν_a NO_2), and 1588 (ν C=C) cm^{-1}. The low-frequency bands at 690 and 774 cm^{-1} correspond to out-of-plane C−H deformations, while the peak at 860 cm^{-1} is due to an in-plane ring breathing vibration coupled with an in-plane phenyl-NO_2 bend. Several important observations can be drawn from Figure 3. (1) In solid NAB the molecules are randomly oriented and both in-plane and out-of-plane vibrations are observed (Figure 3a). (2) For physisorbed NAB, the in-plane bands at 1344 and 1588 cm^{-1} have dramatically decreased absorbance; the only visible contribution in this spectral region is from the asymmetric NO_2 stretch (Figure 3b). On the other hand, the out-of-plane bands of physisorbed NAB exhibit significant intensity (Figure 3c). The spectral characteristics of physisorbed NAB are consistent with the molecule lying flat on the PPF surface. (3) In contrast to physisorbed NAB, the chemisorbed NAB monolayer displays minor out-of-plane contributions as indicated by the weak bands

Table 2. Frequencies and Assignments for Nitroazobenzene

solid[a]	mono-layer	physi-sorbed	Raman	DFT[b] calcn	assignment
690, m	679, w	689, vs		680	γ_s[c] C−H deformation
774, m	774, w	775, s		763	γ_a C−H deformation
860, m	861, w	859, s		837	ν_s (C−NO_2) + ring breathing
			1107	1085	ν (phenyl-NO_2) + adjacent C−H wag
			1141	1126	ν phenyl−NN stretch
1344, vs	1342, vs	1341, w	1341	1337	ν_s (NO_2)
			1404	1397	N=N + ring deformation
1444 w	1452, s	1445, m	1452	1459	δ_a ring deformation + C−N=N
1466, m	1480, s	1464, m		1470	N=N stretch + ring deformation
1489, m	1493, vs	1488, m		1495	N=N stretch + ring deformation
1521, vs	1517, vs	1520, vs		1554	ν_a (NO_2)
1588, m	1586, s		1595	1589	ν (C=C)

[a] vs, very strong; s, strong; m, medium; w, weak. [b] Calculated with density functional theory B3LYP 6-31G*, with 0.9613 frequency scaling factor. [c] γ, out-of-plane; δ, in-plane; ν, stretch; s, symmetric; a, asymmetric.

in the (650−900 cm^{-1}) spectral region. In addition, there is a relative increase in peak intensity for in-plane vibrations in the range 1250−1500 cm^{-1} and a slight decrease for the 1521-cm^{-1} band compared to the solid NAB spectrum. These spectral features are consistent with the NAB molecule oriented upright on the PPF surface. For NAB (1.9) bonded to PPF, eq 2 yields an average tilt angle (α) of 31.0 ± 4.5° with respect to the surface normal, based on the weak out-of-plane C−H mode at 690 cm^{-1} and the in-plane vibration at 1344 cm^{-1}. A similar analysis on the out-of-plane C−H band at 775 cm^{-1} and the in-plane nitro stretch at 1344 cm^{-1} results in an average tilt angle (α) of 27.2 ± 9.3°. These α values were calculated by assuming the rotation angle (ϕ) about the long axis of the molecule is 0°. In principle, the rotation angle could be determined from the intensity of the in-plane mode parallel to the short axis of the molecule compared to that of the out-of-plane mode (eqs 4 and 5). However, the theoretical calculations for NAB indicate that all of the observed short-axis modes are coupled to the asymmetric stretch of the nitro group. This coupling complicates the determination of the rotation angle (ϕ) because the nitro group exhibits large-amplitude torsional flexibility, resulting in a net transition dipole having both short-axis in-plane and out-of-plane components. Regardless, variations in rotation angle (ϕ) up to 30° from the surface plane only alter the calculated average tilt angle (α) by less than 4°, well within the range of the standard deviation of the average tilt angle reported. Only when the rotation angle (ϕ) exceeds 45° does the correction to the average tilt angle become significant. Rotation angles greater than 45° are unlikely because these would imply tilt angles (α) that are sufficiently large that significant steric interactions would occur between NAB and the surface.

A comparison of solid NBP, chemisorbed NBP, and physisorbed NBP on PPF is shown in Figure 4, and observed band frequencies and assignments are listed in Table 3. The major peak at 1346 cm^{-1} is an in-plane vibrational mode whose intensity relative to the 740-cm^{-1} mode is stronger in the chemisorbed NBP monolayer (Figure 4b) than in solid KBr (Figure 4a). Physisorbed NBP has an intense out-of-plane band at 733 cm^{-1} and a smaller band near 877 cm^{-1} (Figure 4c). The in-plane symmetric NO_2

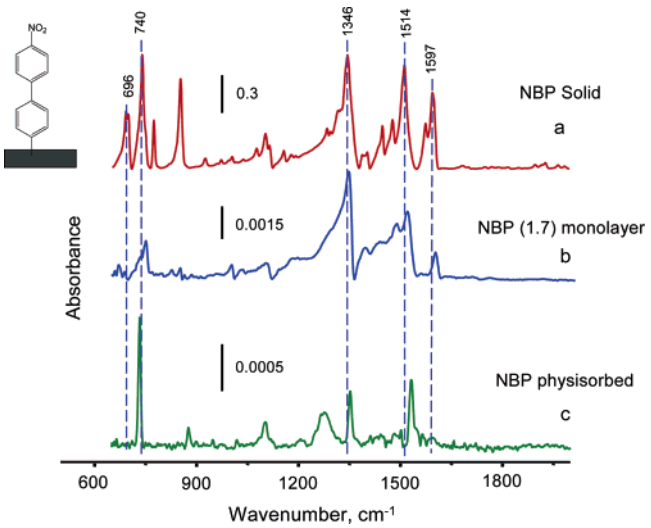

Figure 4. FT-IR spectra of (a) solid NBP in a KBr pellet, (b) the corresponding chemisorbed monolayer 1.7 nm thick, and (c) a physisorbed layer on PPF.

Table 3. Frequencies and Assignments for Nitrobiphenyl

solid[a]	mon-olayer	physi-sorbed	DFT[b] calcn	assignment
696, m	691, w		725	γ_s[c] C−H deformation
740, vs	738, w	733, vs	735	γ_a C−H deformation
774, m	vw		756	γ C−H deformation
854, s	852, w	877 w	835	γ_s C−H deformation + NO_2 breathing
1104,m	1101, w	1103, m	1090	ν (C−NO_2) + adjacent C−H wag
1346, vs	1342, vs	1352, m	1341	ν_s (NO_2)
1449, m	1443, m	1443, w	1445	δ_a ring deformation
1479, m	1482, s	1483	1476	δ_s C−H deformation
1514, s	1513, s	1532, s	1546	ν_a (NO_2)
1597, s	1595, w	1596, w	1601	ν_a (NO_2) + ν (C=C)

[a] vs, very strong; s, strong; m, medium; w, weak. [b] Calculated with density functional theory B3LYP 6-31G*, with 0.9613 frequency scaling factor. [c] γ, out-of-plane; δ, in-plane; ν, stretch; s, symmetric; a, asymmetric.

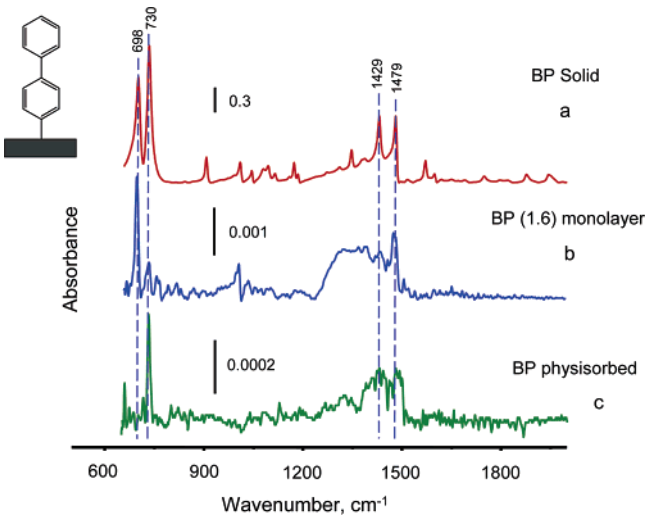

Figure 5. FT-IR spectra of (a) solid BP in a KBr pellet, (b) chemisorbed monolayer 1.6 nm thick, and (c) a physisorbed layer on PPF.

Table 4. Frequencies and Assignments for Biphenyl

solid[a]	monolayer	physisorbed	DFT[b] calcn	assignment
698, s	693, vs		686	γ_s[c] C−H deformation
730, vs	729, w	733 vs	726	γ_s C−H deformation
1005, w	1004, w		989	ring breathing
1429, m	1426, m	1429, m	1431	δ_s ring deformation + C−H wag
1479, m	1475, m	1483, m	1477	δ_a ring deformation + C−H wag

[a] vs, very strong; s, strong; m, medium; w, weak. [b] Calculated with density functional theory B3LYP 6-31G*, with 0.9613 frequency scaling factor. [c] γ, out-of-plane; δ, in-plane; ν, stretch; s, symmetric; a, asymmetric.

stretch is observed as a medium peak at 1352 cm^{-1} while the asymmetric NO_2 stretch band is located near 1532 cm^{-1}, both higher in frequency than the solid and chemisorbed cases, but consistent with the literature on nitro-containing phenyl rings in the gas and liquid phases.[61–63] In addition to the nitro torsional motion, the phenyl rings in the NBP molecule are not coplanar, thus reducing the possibility of the molecule resting flat on the substrate surface. As a result, both out-of-plane and in-plane vibrational modes contribute to the NBP spectrum in all three cases, as shown in Figure 4 and Table 3. Although these complications prevent a definitive calculation of the NBP orientation, there is good evidence that the chemisorbed NBP is oriented approximately perpendicular to the PPF surface as follows: (1) The intensities of the vibrational modes associated with out-of-plane deformations (696−774 cm^{-1}) are significantly diminished in the chemisorbed monolayer. (2) The in-plane symmetric NO_2 stretch near 1346 cm^{-1} is stronger in the chemisorbed monolayer than in the physisorbed sample. (3) The in-plane 1346 cm^{-1}/out-of-plane 740 cm^{-1} ratio is 1.0 for solid NBP and 0.4 for the physisorbed layer, but increases to 4.9 for the chemisorbed monolayer.

Infrared spectra for solid, chemisorbed, and physisorbed BP are shown in Figure 5, with the vibrational modes summarized in Table 4. Chemisorbed BP exhibits increased relative intensity of the in-plane vibrations (1426 and 1479 cm^{-1}) and decreased intensity of the out-of-plane deformation (729 cm^{-1}), relative to the randomly oriented solid. However, determination of the adsorption geometry is complex due to the presence of a dihedral angle between the phenyl rings. As a result, the band at 693 cm^{-1} associated with a symmetric out-of-plane deformation is clearly apparent in the chemisorbed BP spectrum. The in-plane (1479 cm^{-1})/out-of-plane (729 cm^{-1}) ratios for solid and physisorbed cases are both 0.5; while for the chemisorbed monolayer it was 1.8. By contrast, the 1479 cm^{-1}/698 cm^{-1} ratio was estimated to be 0.6 for solid BP in KBr and 0.5 in the BP monolayer but near infinity in the physisorbed spectrum.

FL is a planar derivative of BP, with a near-zero dihedral angle between the phenyl rings. There is only one useful band in the in-plane deformation spectral region (1447 cm^{-1}), as well as one out-of-plane mode (737 cm^{-1}), as illustrated in Figure 6 and Table 5. For FL chemisorbed to PPF, the out-of-plane mode at 737 cm^{-1}

(61) Lin-Vien, D.; Colthup, N.; Fateley, W.; Grasselli, J. *The Handobook of Infrared and Raman Characteristic Frequencies of Organic Molecules*; Academic Press: San Diego, 1991.
(62) Roeges, N. *A Guide to the Complete Interpretation of Infrared Spectra of Organic Structures*; John Wiley & Sons: Chinchester, 1994.
(63) Nyquist, R. A. *Interpreting Infrared, Raman, and Nuclear Magnetic Resonance Spectra*; Academic Press: San Diego, 2001.
(64) Ou, R.; Samuel, R. *J. Polym. Sci.* **1999**, *37*, 3473.

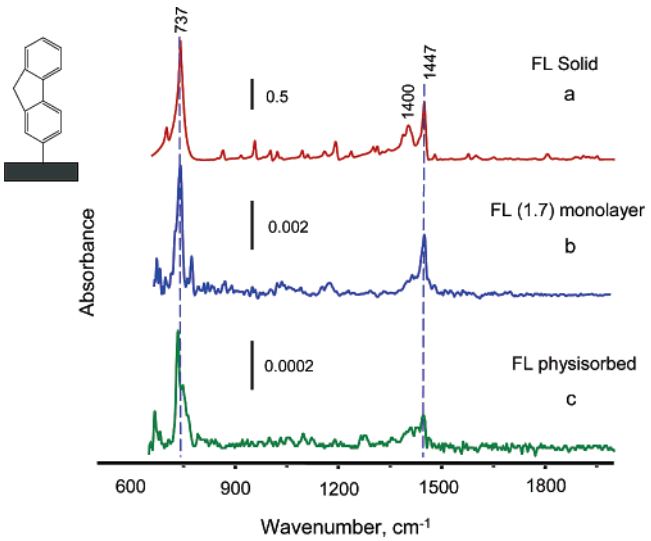

Figure 6. FT-IR spectra of (a) solid FL in a KBr pellet, (b) chemisorbed monolayer 1.7 nm thick, and (c) physisorbed layer on PPF.

Table 5. Frequencies and Assignments for Fluorene

solid[a]	monolayer	physi-sorbed	DFT[b] calcn	assignment
737, vs	731 vs	734 vs	730	γ_s[c] all C−H deformation
1400, m	1402, w	1401, w	1423	$-CH_2$ scissoring
1447, m	1451, m	1447, m	1445	δ_s ring deformation and C−H wag

[a] vs, very strong; s, strong; m, medium; w, weak. [b] Calculated with density functional theory B3LYP 6-31G*, with 0.9613 frequency scaling factor. [c] γ, out-of-plane; δ, in-plane; ν, stretch; s, symmetric; a, asymmetric.

and the in-plane vibration at 1447 cm^{-1} yielded an averaged tilt angle (α) of 44.2 ± 5.4° with respect to the surface normal, based on eq 2.

Raman Spectroscopy. Mono- and multilayers of NAB and AB and films of PANI were examined with Raman spectroscopy using both p- and s-polarized incident laser light. Raman spectra for different incident laser polarizations for NAB on PPF are shown in Figure 7. The peaks at 1402 and 1452 cm^{-1} are associated with N=N stretching modes while the band near 1341 cm^{-1} corresponds to the symmetric NO_2 stretch. All of the observed Raman bands are resonance enhanced, so it is reasonable to expect the maximum intensity for an incident electric field parallel to the long axis of the NAB molecule, when the electric−dipole interaction is maximized.[50] As observed in Figure 7a and b, when the incoming laser beam is at 75° from the surface normal, p-polarized light provides a stronger signal than s-polarized radiation for both NAB (4.5) and NAB (1.9). At a lower angle of incidence (Figure 7c and d), both the multilayer and monolayer display the same intensity for s- or p-polarized light. A similar result was obtained for mono- and multilayers of AB, shown in Figure 8, whereby p-polarized light at 75° provides greater intensity than s-polarized while at 0° there is no marked intensity difference for s- and p-polarized radiation. Raman results for 15 samples of NAB on PPF are summarized in Table 6, as the observed ratio of the 1140-cm^{-1} band intensity for p-polarized to s-polarized laser light at three angles of incidence. For glancing incidence (75°), p-polarized laser light consistently yielded more intensity for chemisorbed

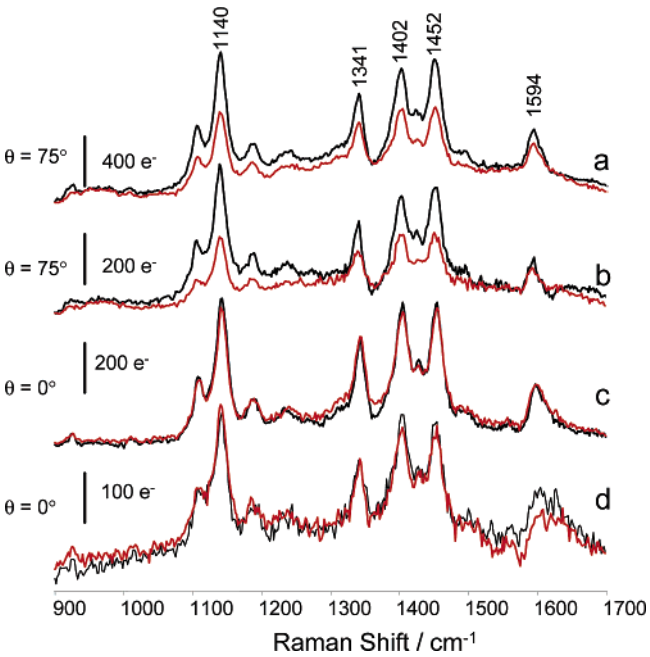

Figure 7. Raman spectra of chemisorbed NAB (a) multilayer (75°), (b) monolayer (75°), (c) multilayer (0°), and (d) monolayer (0°). Angles are relative to the surface normal. Black spectra are for p-polarized and red spectra are for s-polarized laser light. Scale bars represent relative intensities, in terms of CCD detector counts.

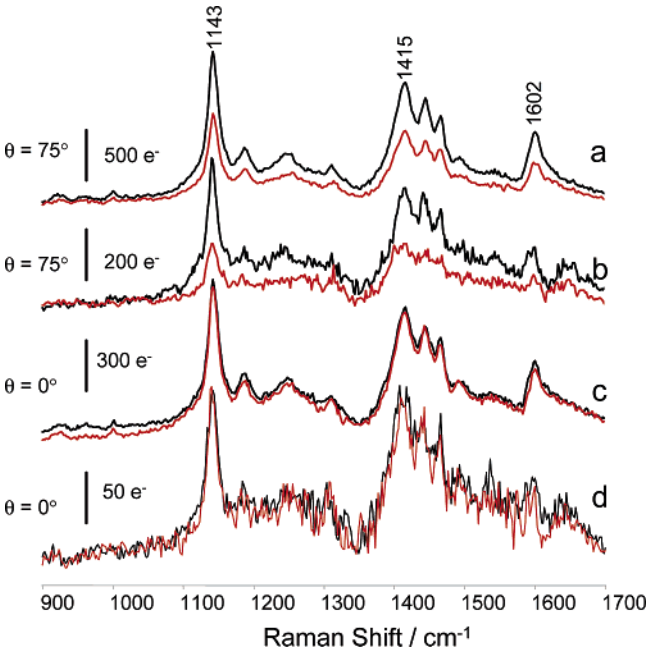

Figure 8. Raman spectra of AB (a) multilayer (75°), (b) monolayer (75°), (c) multilayer (0°), and (d) monolayer (0°). Angles are referenced against the surface normal. Black spectra are for p-polarized and red spectra are for s-polarized laser light. Scale bars represent relative intensities, in terms of CCD detector counts.

NAB than s-polarized light, while essentially no difference was observed for 0° incidence. For spin-coated NAB from 1 to 4 mM solutions, the opposite was true, with s-polarized light yielding consistently higher Raman intensity at 75° but negligible difference between s- and p-polarized at 0°.

Spectra for NAB physisorbed to PPF by spin coating are shown in Figure 9b and c and compared to solid NAB in Figure 9a. NAB

Table 6. Raman Intensity Ratios for the 1140-cm^{-1} Band for Various NAB Samples on PPF I_p/I_s (1140 cm^{-1})[a]

laser incidence angle	75°	45°	0°
chemisorbed NAB (1.9[b]) $N = 6$[c]	1.99 ± 0.37	1.18 ± 0.09	1.01 ± 0.06
chemisorbed NAB (4.5) $N = 5$	1.69 ± 0.20	1.49 ± 0.55	1.02 ± 0.03
spin-coated NAB, 1 mM[d]	0.46	0.74	1.02
3 mM	0.82	0.96	0.90
4 mM	0.64	0.88	0.98
5 mM	1.80	1.11	1.12
mean ± SD[e]	0.64 ± 0.18	0.86 ± 0.11	0.97 ± 0.06

[a] Ratio of intensity for p-polarized incident laser light to that for s-polarized, for 1142-cm^{-1} Raman band, stated as mean ± standard deviation. [b] Number in parentheses indicates thickness in nm, determined by AFM. [c] Number of independent samples. [d] Concentration of NAB spin coated at 4000 rpm for 10 s. [e] For 1−4 mM range.

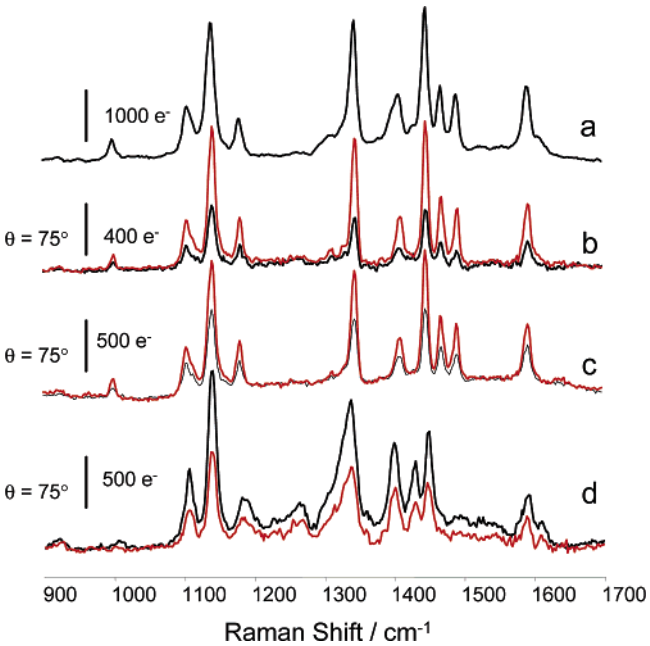

Figure 9. Raman spectra of NAB (a) solid and spin-coated nitroazobenzene of concentrations (b) 1, (c) 4, and (d) 5 mM at 4000 rpm for 10 s at 75°. Angles are referred against the surface normal. Black spectra are for p-polarized and red spectra are for s-polarized laser light. Scale bars represent relative intensities, in terms of CCD detector counts.

physisorbed from 1 to 4 mM solution exhibited significantly higher intensity for s-polarized light than for p-polarized light for a 75° incidence angle Spectra of NAB spin coated at high concentration (5 mM, Figure 9d) differed from those at lower concentration, presumably due to aggregation and disordering of the physisorbed film. To verify that the observed polarization effects are not a consequence of the PPF or observation geometry, PANI films were prepared by electropolymerization on PPF. Once a PANI film is more than a few nanometers thick, the polymer chains would be expected to be randomly oriented with respect to the PPF surface. As shown in Figure 10, there is no significant difference in the Raman intensities for p- and s-polarized incident laser light for either 75° or normal incidence, once the polyaniline film reaches a thickness of 60 nm.

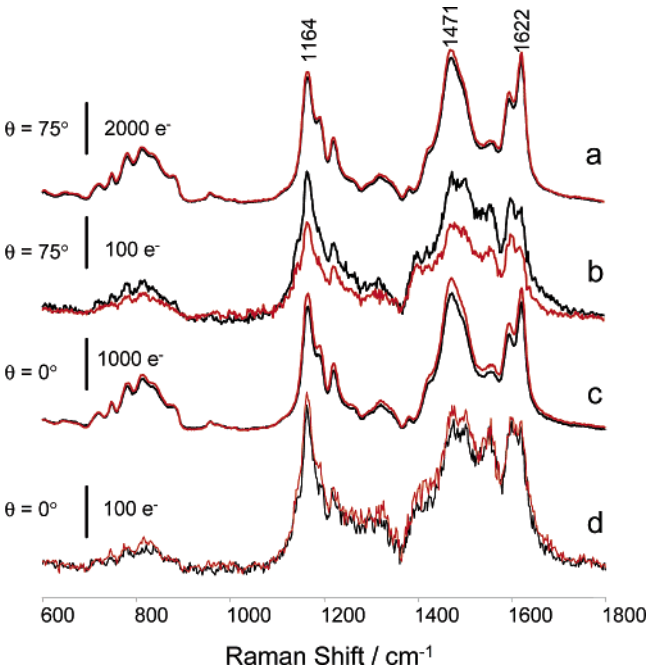

Figure 10. Raman spectra of PANI (a) 50-nm-thick film (75°), (b) 6-nm film (75°), (c) 50-nm film (0°), and (d) 6-nm film (0°). Angles are referenced against the surface normal. Black spectra are for p-polarized and red spectra are for s-polarized laser light. Scale bars represent relative intensities, in terms of CCD detector counts.

DISCUSSION

The studies herein indicate that IR spectra of organic molecules chemisorbed onto a flat carbon substrate can be obtained with monolayer sensitivity. The quality of the spectra is comparable to that previously reported for porphyrin structures tethered to silicon.[43−45] The larger dipole change associated with vibrations of the nitro group results in stronger absorption for the nitro-containing adsorbates (NAB and NBP), compared to those lacking this functionality (BP and FL). The ability to obtain useful IR spectra for ~1.7-nm-thick monolayers is somewhat surprising given that 7.8 nm of polymer was required to observe IR absorptions on GC using an external reflection geometry.[49] The improved sensitivity of the current work may be due to an optical advantage of the GATR configuration or to the flatter and more regular surface of PPF compared to GC. However, the sensitivity was not sufficient to characterize the phenyl−surface C−C bond, due to interference from the relatively high density of C−C bonds in the PPF surface. The similarity of the chemisorbed IR spectra to that of the isolated molecules indicates that the molecules are not significantly modified structurally upon attachment to the surface. The absence of the N≡N stretch around 2130−2300 cm^{-1} indicates complete loss of the diazonium group by radical formation and subsequent chemisorption to the PPF surface, by either addition to aromatic C=C bonds or coupling to radical centers on the graphitic edge plane. The origin of the broad IR absorptions in the 1250−1500-cm^{-1} range, which are most prominent in the chemisorbed samples, is not clear. The fact that similar features are not apparent with silicon or metal substrates implies that they may be due to C−C vibrations in the graphitic surface, which are "activated" by the chemisorption reaction.

As noted in the introduction, the orientation of the molecules relative to the surface is deduced from the IR absorption intensity

by the relationship between the incident electric field and the dipole derivative vector and does not depend on cancellation of the s-polarized light intensity within the carbon substrate. For all of the chemisorbed molecules in the current investigation, the in-plane vibrational modes show stronger absorptions than the out-of-plane modes, consistent with a more upright orientation on the surface. The average tilt angles, which could be determined for both NAB and FL, provide further support for this adsorption geometry. While the average tilt angles yield information on the average geometry of the chemisorbed molecules, they provide no details about the polar angle around the surface normal and the rotation around the main molecular axis with respect to the surface plane. In other words, the molecules are most likely randomly rotated around the surface−phenyl bond, and phenyl−phenyl bond in the case of NBP and BP. The spectra of physisorbed molecules provide important contrasts to the chemisorbed case, with much stronger out-of-plane modes indicating that the physisorbed molecules lie predominantly flat on the PPF surface. The fact that the chemisorbed and physisorbed molecules show large differences in relative intensity for in-plane and out-of-plane vibrations clearly indicates that the two cases have different orientations of the molecular axis to the surface. If the chemisorbed or physisorbed molecules were oriented randomly, the relative intensities should be similar to the isotropically oriented molecules in the solid (KBr) samples.

The Raman scattering characteristics of NAB and AB provide further support for an upright orientation of the molecules in the monolayers. The fact that both the NAB and AB chemisorbed monolayers exhibit a higher ratio of Raman intensity of p-polarized light to that for s-polarized is consistent with an orientation with the long axes of the molecules preferentially parallel to the surface normal. Despite the added complexity of resonance enhancement, several observations are consistent with the presumption that the Raman intensity is maximized when the electric field vector of the incident light is parallel to the long axis of the molecule. First, physisorbed NAB and AB, which are expected to lie flat on the PPF surfaces, show small relative intensity ratios, with s-polarized light yielding more Raman scattering than p-polarized. For s-polarized light, the electric field vectors will be parallel to the long axis of a subset of physisorbed molecules. Second, randomly oriented PANI shows no difference in Raman intensity from p- or s-polarized laser light for either normal or glancing incidence, provided the PANI film is thick enough to be isotropic. Finally, we note that a relatively upright orientation for the NAB and AB monolayers is consistent with the AFM determined layer thickness, i.e., close to the length of one molecule bonded to the PPF, including the van der Waal radius of the terminal atom.[32] Collectively, the IR, Raman, and AFM measurements for the NAB and AB monolayers, as well as NBP, BP, and FL monolayers, indicate a more upright adsorption geometry for the chemisorbed molecules.

The current studies further reveal that the spectral characteristics of the NAB and NBP multilayers are similar to those of the monolayers with respect to the relative intensities of the in-plane and out-of plane vibrations. Apparently the second and subsequent layers of the multilayer are not completely disordered, possibly because radical attack occurs at the ortho position to the nitro group of the first layer. A similar multilayer formation mechanism was reported by Kariuki and McDermott for diethylaminophenyl diazonium reduction on GC and pyrolytic graphite.[5,6]

We have previously reported on the electrical properties of monolayers of NAB,[25] NBP, BP, and FL in PPF/molecule/Cu molecular junctions,[25,29] in which observed differences in conductivity were attributed to a strong dependence on molecular structure rather than an artifact of junction fabrication. Given that PPF is flat but disordered, there was uncertainty about the alignment of the surface-bound molecules relative to the PPF surface. The current spectroscopic studies confirm that NAB, NBP, BP, and FL are oriented with their long axes relatively upright with respect to the surface normal, as was assumed (but not proven) in earlier reports and implied by AFM measurements.[32] Molecular junctions of the same thickness and area (0.000 45 cm^2) made from NBP, FL, and BP monolayers had observed resistances of 286, 886, and 9890 Ω, respectively.[29] Given the current conclusion that the orientations of these molecules on PPF are similar, it is very unlikely that the factor of 35 range of observed conductance is a consequence of differences in orientation. Rather, the results support the original conclusion that the wide range of molecular junction conductivity is a consequence of differences in molecular structure, particularly the dihedral angle between phenyl rings and the presence of the nitro group.

CONCLUSIONS

The findings reported herein indicate that organic molecules tethered to flat carbon surfaces can be characterized by attenuated total reflectance infrared spectroscopy, which can reveal valuable information on structure and molecular orientation. The Ge ATR accessory provides monolayer sensitivity for organic monolayers bonded to a very flat carbon surface, without the surface selection rule normally operative with metal substrates. The study demonstrates that electroreduced aryldiazonium molecules retain their integrity upon surface attachment, with the exception of the expected loss of the N_2^+ functional group. The chemisorbed molecular layers do not lie flat on the substrate, but rather chemisorb preferentially with their long axes approximately parallel to the surface normal. This geometry is consistent with previous, less direct determination based on voltammetry and atomic force microscopy. Current work is underway to obtain spectroscopic information of the chemisorbed organic monolayers through thin metal films. Of particular interest is whether IR spectra can be obtained in a finished molecular junction to determine the state of the adsorbed molecule both after metal deposition and under an applied bias.

ACKNOWLEDGMENT

This work was supported by the NSF Analytical and Surface Chemistry Division (R.L.M.), DARPA/DMEA (D.F.B.), and by ZettaCore, Inc (R.L.M. and D.F.B.).

Received for review November 17, 2005. Accepted February 20, 2006.

AC052042H